Simulation-time Reduction Techniques for a Retrofit Planning Tool

Georgios I. Giannakis[1], Georgios D. Kontes[2], Ivan Korolija[3], Dimitrios V. Rovas[3]
[1]School of Production Engineering & Management, Technical University of Crete, Greece
[2]Technische Hochschule Nürnberg & Fraunhofer IBP, Nuremberg, Germany
[3]Institute for Environmental Design and Engineering, University College London, UK

Abstract

The design of retrofitted energy efficient buildings is a promising option towards achieving a cost-effective improvement of the overall building sector's energy performance. With the aim of discovering the best design for a retrofitting project in an automatic manner, a decision making (or optimization) process is usually adopted, utilizing accurate building simulation models towards evaluating the candidate retrofitting scenarios. A major factor which affects the overall computational time of such a process is the simulation execution time. Since high complexity and prohibitive simulation execution time are predominantly due to the full-scale, detailed simulation, in this work, the following simulation-time reduction methodologies are evaluated with respect to accuracy and computational effort in a test building: Hierarchical clustering; Koopman modes; and Meta-models. The simplified model that would be the outcome of these approaches, can be utilized by any optimization approach to discover the best retrofitting option.

Introduction

Following the recast of the Energy Performance of Buildings Directive (EPBD), in recent studies, the retrofitting of existing buildings is considered as a promising option towards achieving a cost-effective improvement of the overall building sector's energy performance. With the aim of discovering the best design for a retrofitting project, a decision-making or an optimization process is adopted, where repeated evaluation of different candidate designs is required. Commonly, for each design evaluation, a respective, accurate building simulation model is developed and executed, making the overall decision-making (or optimization) process a quite laborious and time consuming task.

The major factor affecting the overall computational time of such a repeated evaluation process is the simulation execution time. Since high complexity and prohibitive simulation execution time are predominantly due to the full-scale, detailed, geometry representation of the building, geometry reduction methodologies (Giannakis et al., 2013) can be applied. The effectiveness of such methodologies relies on the modeler experience and the building's shape, hence an automatic process to generate speedup models by applying geometry reduction methodologies is unfeasible.

In recent studies (Lilis et al., 2016; Bazjanac, 2008), methodologies for semi-automated Building Energy Performance (BEP) simulation model generation, utilizing Building Information Model (BIM) data, are introduced. These methodologies make the BEP simulation model generation process much more expedient, however a characteristic of the full-scale thermal simulation models generated is that they treat each room of a building as an individual thermal zone. This assumption increases significantly the simulation runtime, since computational effort is more than proportional to the number of zones, as increased number of zones corresponds to increased number of ordinary differential equations to be solved. Hence, in many cases, building simulation modelers follow the HVAC zones definition and each HVAC zone is a thermal zone (ASHRAE 90.1, 2010), but even using this simplification the resulting simulation model can still be computationally expensive. Concerning further zoning reduction, building simulation experts are able to reduce the number of HVAC-thermal zones, but such a reduction is usually based on some similarity between the regions being combined (ASHRAE 90.1, 2010) (e.g. similar internal loads). Towards an automatic process to reduce the number of thermal zones, in the present work two zoning reduction methodologies are investigated. The first one utilizes the Hierarchical Clustering theory (Maimon and Rokach, 2005), while the second one adopts the Koopman modes theory (Georgescu and Mezić, 2015).

Other simulation-time reduction techniques try to reduce the number of expensive simulation calls utilizing surrogate models, called meta-models, for estimating e.g. the energy consumption of each candidate solution. Meta-models are pre-trained using data from a small number of simulations, and are then used to evaluate candidate solutions without directly interfacing with the computationally expensive simulation tool during the decision making (or optimization) process.

Several different types of meta-models (or surrogates) have been defined in the literature (e.g. see (Forrester et al., 2008) for an overview), but for the task at hand, the most common choices are Support Vec-

tor Machines (SVM) (Symonds et al., 2016), Neural Networks (NN) (Symonds et al., 2016; Magnier and Haghighat, 2010) and Gaussian Processes (GPs) (Zhang et al., 2013; Safarzadegan Gilan et al., 2016).
In this work, we have selected to use non-parametric regression models for constructing the meta-models. Here, in contrast to parametric models that assume a fixed model structure (like e.g. the number of nodes and hidden layers in a NN), thus bounding the expressiveness of the model, non-parametric models assume an infinite-dimensional vector of parameters (Scholkopf and Smola, 2001), where the amount of information that can be captured from the model grows (up to a certain degree) as the amount of data grows. In addition, non-parametric models allow us to use the same models in all the experimental setups, regardless of the type of the building, the specifics of the HVAC system, the modeled quantity (e.g. energy consumption or user comfort), etc., whereas in the case of parametric models, a laborious manual model selection process has to be performed.
Among the two types of non-parametric models, we utilize GPs for the modeling task at hand. Despite the fact that both methodologies have the capacity to model complex functions, GPs offer an uncertainty estimate in each test point, thus enabling a more informative search in the parameter space (Zhang et al., 2013; Safarzadegan Gilan et al., 2016).
Summarizing, in the present work, the three aforementioned methodologies (Hierarchical Clustering, Koopman modes and GP meta-models) are evaluated with respect to accuracy and computational effort in a test building. The simplified model that would be the outcome of these approaches, can be utilized by any of the optimization approaches that have been proposed in the literature for discovering optimized retrofitting options – with this evaluation being part of our future research.

The methodologies

Hierarchical clustering

Hierarchical clustering is a method of cluster analysis which seeks to build a hierarchy of clusters. Hierarchical clustering strategies are divided into agglomerative and divisive. Given a data-set consisting of a number of objects ("object" term is taken from how EnergyPlus defines different instances of the Output:Variable class) – for example, time-series of thermal zones' air temperatures, derived from a thermal model simulation for a predefined simulation run-period – the agglomerative technique considers that each object starts in its own cluster and pairs of clusters are merged at each step, until all objects are placed in one cluster (bottom-up). The divisive technique works vice versa; assuming that all objects belong to a cluster, it divides this cluster until each cluster contains a unique object (top-down).
Here, the agglomerative strategy for hierarchical clustering is adopted, since considering a large number of thermal zones, a reduced number of thermal zones must be obtained.
In a broad sense, the agglomerative technique is performed as follows (Maimon and Rokach, 2005):

1. A single cluster is defined for each object of the data-set; for instance, if there is a set of n_x objects to be merged, there are n_x clusters, where each cluster contains an object of n_x;
2. The similarity or dissimilarity between every pair of objects in the data set is estimated; here, the pairwise distance between pairs of objects is calculated. Some commonly norms (metrics) to compute this distance are: Euclidean, Squared Euclidean, and Maximum distances.
3. The pair with the minimum distance is selected; this pair is merged into one cluster, leading to newly formed clusters.
4. The newly formed clusters are grouped into larger clusters until a hierarchical tree is formed. To calculate the distance between clusters that include more than one objects a linkage criterion is selected. The linkage criterion determines the distance between sets of objects as a function of the pairwise distances between objects. Some commonly used linkage criteria between two sets of objects are: Maximum, Minimum and Average linkages.
5. Finally, the point to cut the hierarchical tree into clusters is determined. In this step, branches off the bottom of the hierarchical tree are pruned, and all objects below each cut are assigned to a single cluster.

The choice of an appropriate metric (in step 2.) will influence the shape of the clusters, as some elements may be close according to one distance and further away according to another.
To explain the aforementioned metrics and linkage criteria, suppose that we have a data-set represented as a matrix $G \in \mathbb{R}^{n_x, n_{\text{data}}}$, where n_x stands for number of objects (e.g. n_x zones' air temperature time-series) and n_{data} stands for the number of time steps when the values were measured. Moreover, two clusters A and B are considered. Cluster A consists of n_A objects where each of them is element of $\{1, 2, \ldots, n_A\}$, while cluster B consists of n_B objects $\{B_1, B_2, ..., B_{n_B}\}$, where $n_A + n_B \leq n_x$. The distance $\delta_{i,j}$ between objects $i \in A$ and $j \in B$ according to the Euclidean distance, can be calculated by the following equation:

$$\delta_{i,j} = \sqrt{\sum_{k=1}^{n_{\text{data}}} (G_{i,k} - G_{j,k})^2}. \quad (1)$$

According to the Averaged linkage criterion, the distance between cluster A and cluster B, δ_{AB}, is defined

as follows:

$$\delta_{AB} = \frac{\sum_{i \in A} \sum_{j \in B} \delta_{i,j}}{n_A \cdot n_B}. \quad (2)$$

In the present work, the choice of linkage criterion is not of high importance, since the point to cut the hierarchical tree into clusters is defined as the point where the zones' pair with the minimum distance are linked. Such a definition stems from the following interpretation: when two thermal zones are merged into a new one, the new zone's resulting temperature profile could be conspicuously different from the temperature profiles of the initial zones; hence, the data-set should be updated whenever a two zones' merging is performed. To accomplish this, the agglomerative technique is performed repeatedly in the following manner: (1) Set the desired number of zones; (2) Consider a data-set consisting of time-series, derived from the full-scale zonal model simulation; (3) Apply the agglomerative technique, where the point to cut the hierarchical tree into clusters is defined as the point where the zones' pair with the minimum distance are linked; (4) Create a newly formed zonal model according to the results of step 3 and simulate it to receive the updated data-set; (5) Using the updated data-set, repeat steps 3 and 4, until the number of zones is equal to the desired one.

Koopman modes

Since the equations describing a building model can be of a high dimension and are often not accessible analytically, measurement's, or time-series', based methods are required to study such systems. In this context, the Koopman operator can be applied to building models for the visualization and analysis of these systems. By projecting the data-set (time-series of simulated objects) from a building simulation onto eigenfunctions of the operator, spatial features of the system being studied can be extracted.

The procedure of merging thermal zones from a full-scale model using Koopman modes is:

1. Simulate the full-scale thermal simulation model resulting to an objects' data-set of interest (in this work thermal zones' air temperatures).
2. Calculate Koopman eigenvalues and modes by projecting the objects' data-set onto eigenfunctions of the Koopman operator.
3. Merge thermal zones with Koopman modes of similar amplitude and phase at frequencies (modes) of interest.

There are several methods available for calculating Koopman modes (Mezić, 2005; Susuki and Mezic, 2010). Here, Arnoldi algorithm (Susuki and Mezic, 2010) is selected, since in (Georgescu and Mezić, 2015) it is presented as an efficient algorithm to decompose building simulation time-series into Koopman modes, able to capture the thermal behavior of a building. Arnoldi algorithm is described below.

Suppose again that we have the data matrix G as introduced above. Then, empirical Ritz values (Koopman eigenvalues) λ_k and empirical Ritz vectors (Koopman modes, eigenfunctions) v_k, $\forall k = 1, 2, \ldots, n_{\text{data}}$ are calculated by the following procedure:

1. Find constants c_k, $\forall k = 1, \ldots, n_{\text{data}} - 1$ such that $\boldsymbol{r} \perp G$, where:

$$\boldsymbol{r}_i = G_{i,n_{\text{data}}} - \sum_{i=1}^{n_{\text{data}}-1} c_i G_{i,k}. \quad (3)$$

for all $i = 1, \ldots, n_x$. Since $\boldsymbol{r} \perp G$ the following equation holds:

$$G'_{\bullet,k} \boldsymbol{r} = 0 \quad (4)$$

for all $k = 1, \ldots, n_{\text{data}} - 1$ where $G_{\bullet,k}$ stands for kth column of matrix G. Suppose that $A = \{a_{k,\tilde{k}}\} \in \mathbb{R}^{n_{\text{data}}-1, n_{\text{data}}-1}$, where $a_{k,\tilde{k}} = G'_{\bullet,k} G_{\bullet,\tilde{k}}$ and $b_k = G'_{\bullet,k} G_{\bullet,n_{\text{data}}}$ and $c = \{c_i\} \in \mathbb{R}^{n_{\text{data}}-1}$. Then, constants c_k can be found by solving the following system of linear equations:

$$Ac = b \quad (5)$$

2. Define the companion matrix C:

$$C = \begin{bmatrix} 0 & 0 & \cdots & 0 & c_1 \\ 1 & 0 & \cdots & 0 & c_2 \\ 0 & 1 & \cdots & 0 & c_3 \\ \vdots & \vdots & \ddots & \vdots & \vdots \\ 0 & 0 & \cdots & 1 & c_{n_{\text{data}}-1} \end{bmatrix} \quad (6)$$

and find its eigenvalues λ_k, $\forall k \in \{1, 2, \ldots, n_{\text{data}} - 1\}$.

3. Define the Vandermonde matrix T as follows:

$$T = \begin{bmatrix} 1 & \lambda_1 & \lambda_1^2 & \cdots & \lambda_1^{n_{\text{data}}-2} \\ 1 & \lambda_2 & \lambda_2^2 & \cdots & \lambda_2^{n_{\text{data}}-2} \\ \vdots & \vdots & \vdots & \ddots & \vdots \\ 1 & \lambda_{n_{\text{data}}-1} & \lambda_{n_{\text{data}}-1}^2 & \cdots & \lambda_{n_{\text{data}}-1}^{n_{\text{data}}-2} \end{bmatrix}. \quad (7)$$

4. Finally, calculate the matrix $V = GT^{-1}$, columns of which are the Koopman modes. Note that V might contain complex numbers because of inversion of T.

From the calculated Koopman modes of a full-scale building model data, thermal zones are merged if their amplitudes and phases of the Koopman modes considered are within some tolerance. The following definition is used for comparing the amplitudes and phases of zones and creating merged zones approximations:

Select $\epsilon_1, \epsilon_2 \geq 0$ and consider $i, j \in \{1, 2, ..., n_x\}$, while the data' objects are the n_x zones' air temperatures. Then, zones i and j can be merged if:

$$||v_{i,k}|| - ||v_{j,k}|| < \epsilon_1 \quad (8)$$

$$\angle v_{i,k} - \angle v_{j,k}| < \epsilon_2 \quad (9)$$

for all the k-th Koopman modes of interest where $||\cdot||$ stands for absolute value of a complex number and $\angle$ stands for phase of a complex number. Koopman modes of interest correspond to the largest modes, calculated in Step 4. The main idea of investigating the validity of Equations 8 and 9 for Koopman modes of interest, and not all Koopman modes, is based on the fact that only several modes are required to describe important characteristics of the building's thermal response.

GP meta-models

A GP is a collection of random variables, any finite number of which have a joint Gaussian distribution, it is completely specified by its mean function ($m(x)$) and covariance function ($k(x, x')$) and defines a prior on the space of functions ($f(x) \sim \mathcal{GP}(m(x), k(x, x'))$) (Brochu et al., 2009). As stated in (Brochu et al., 2009), intuitively we can consider that a GP is analogous to a function, but instead of returning a scalar $f(x)$ for every x, it returns the mean and variance of a normal distribution over the possible values of f at x.

Let's assume a training dataset $\mathcal{D}$ consisting of l training pairs of $[(x_1, y_1), \ldots, (x_l, y_l)]$, with $x \in \mathbb{R}^d$ and $y \in \mathbb{R}$ and a zero mean function. If we want to sample from the prior, we sample the values of the function at $\mathbf{x}_{1:l}$ to produce the pairs $(\mathbf{x}_{1:l}, \mathbf{f}(x_{1:l}))$. These function values are drawn according to a multivariate normal distribution $\mathcal{N}(0, \mathbf{K})$, where the kernel (or covariance) matrix is given by (Brochu et al., 2009):

$$\mathbf{K} = \begin{bmatrix} k(x_1, x_1), & \ldots, & k(x_1, x_l) \\ \vdots & \ddots & \vdots \\ k(x_l, x_1), & \ldots, & k(x_l, x_l) \end{bmatrix}. \tag{10}$$

Now, if we want to evaluate the value $f(x_{l+1})$ of a new point x_{l+1}, then $\mathbf{f}(x_{1:l})$ and $f(x_{l+1})$ are jointly gaussian:

$$\begin{bmatrix} \mathbf{f}(\mathbf{x}_{1:l}) \\ f(x_{l+1}) \end{bmatrix} \sim \mathcal{N}\left(\mathbf{0}, \begin{bmatrix} \mathbf{K} & \mathbf{k} \\ \mathbf{k}^T & k(x_{l+1}, x_{l+1}) \end{bmatrix}\right), \quad \mathbf{k} = [k(x_{l+1}, x_1), \ldots, k(x_{l+1}, x_l)]. \tag{11}$$

From here, we can derive the predictive distribution:

$$\begin{aligned} P\left(f(x_{l+1})|\mathcal{D}, x_{l+1}\right) &= \mathcal{N}\left(\mu_l(x_{l+1}), \sigma_l^2(x_{l+1})\right), \\ \mu_l(x_{l+1}) &= \mathbf{k}^T\mathbf{K}^{-1}f(x_{1:l}) \\ \sigma_l^2(x_{l+1}) &= k(x_{l+1}, x_{l+1}) - \mathbf{k}^T\mathbf{K}^{-1}\mathbf{k}. \end{aligned} \tag{12}$$

The choice of covariance function for the Gaussian Process determines the smoothness properties of the underlying function. The simplest and most commonly used is the Squared Exponential (SE) covariance function, defined as:

$$k_{\text{SE}}(x, x') = \exp\left(-\frac{||x - x'||^2}{2d^2}\right), \tag{13}$$

with d a *hyperparameter* that controls the width of the kernel. Another typical covariance function is the Rational Quadratic (RQ), defined as:

$$k_{\text{RQ}}(x, x') = \left(1 + \frac{||x - x'||^2}{2ad^2}\right)^{-a}, \tag{14}$$

with $d, a > 0$ the hyperparameters. This covariance function is equivalent to an infinite sum of squared exponential covariance functions with different length-scales d. Finally, an important class of covariance functions, which are less smooth compared to the SE and RQ, are the Matérn covariance functions, defined as follows:

$$k_{\text{Matern}}(x, x') = \frac{2^{1-\nu}}{\Gamma(\nu)}\left(\frac{\sqrt{2\nu}||x - x'||}{d}\right)^{\nu} H_\nu\left(\frac{\sqrt{2\nu}||x - x'||}{d}\right), \tag{15}$$

with $\nu, d > 0$ the hyperparameters and $\Gamma(\nu)$ and H_ν the Gamma and Bessel functions of order ν respectively.

Apart from the above, a plethora of covariance functions are available (Rasmussen and Williams, 2006), while it is also possible to design new covariance functions by combining existing ones (Duvenaud et al., 2013).

Simulation and experiments

Simulation set-up

Test case this study is based on an office building, depicted in Figure 1. Its full-scale simulation model is formed of 25 thermal zones each accompanied with a detail specifications of activities, schedules, internal gains and thermostat setpoints.

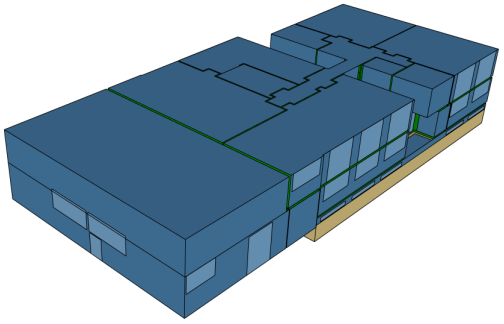

Figure 1: Test building – full-scale simulation model geometry

For the building's geometry creation, an automated BIM to BEP transformation process (Giannakis et al., 2015) was implemented on the geometrical three dimensional data of the test building (see Figure 2).

To define a considerable number of retrofitting scenarios that closely matches real-cases, variability in the model inputs has been performed by parameterizing certain model components which can be grouped

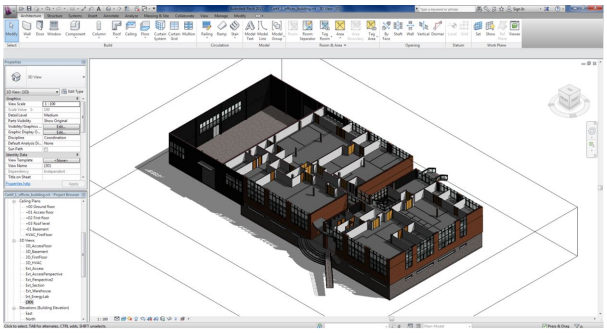

Figure 2: Test building – BIM in Revit 2014

in three categories: building related parameters, activities related parameters and HVAC system related parameters. The selection of building related parameters and activities related parameters parameters has been thoroughly discussed in (Korolija et al. 2013b), while the summary information is provided here for the convenience of the readers.

Building components which were parameterized are building fabric, glazing type and overhang sizes. Building fabric represents a thermally medium weight structure with a concrete as a core material. Thermal performance of the structure was modulated by varying the thickness of insulation layer starting from completely uninsulated building. Five types of building fabric (BF) were included starting from the uninsulated fabric (BF1). U-values of the most important fabric elements are presented in Table 1. Five types of glazing were allowed to be changed independently of building fabric. In addition to the single 4mm clear glass pane, four double glazing types were specified as a design option: two types made of 4mm clear glass panes with a air filled gap of 6mm and 12mm respectively and two types made of 4mm clear glass outer pane and 4mm Low-E inner pane with a main difference of the type of gas used to fill the cavity; air or xenon. Three depths of overhangs above windows were included in analysis (40cm, 80cm and 1.2m) in addition to the option with no overhangs at all. Varying an overhang depth was limited per facade orientation. Building air tightness was specified by infiltration rate (in air changes per hour - ACH) at 0.1 ACH, which represents a very airtight building.

Table 1: Building fabrics (BF) U-values

Build element	**U-Value** $[W/m^2K]$				
	BF1	BF2	BF3	BF4	BF5
External wall	1.62	0.54	0.40	0.32	0.24
Roof	2.48	0.43	0.31	0.17	0.14
Ground floor	1.03	0.82	0.34	0.25	0.14

Internal gains from office equipment and artificial lighting were set to 10 W/m^2 and 4 W/m^2, respectively. It has been assumed that both the equipment and lighting are active during occupied period only.

The analyzed building was assumed to be fully air-conditioned where the type of Heating, Ventilating and Air-Conditioning (HVAC) system was one of the following: Variable Air Volume flow rate system (VAV), Constant Air Volume flow rate system (CAV) and Fan-coil system (FC) with a dedicated fresh air supply. Technical details of each of these systems, including the associated control, have been described in details by (Korolija et al. 2013a). Fresh air requirements were defined per occupant and were met by fixing the minimum fresh air flow rate to 15 liters/s/p. The system is controlled by a dual set-point temperature sensor, where heating and cooling set-point temperatures were set to 21°C and 23°C, respectively.

Table 2: Parameter list and values of the different retrofitting options

Parameter	**Value**
Systems	$\{VAV, CAV, FC\}$
Overhand Depth North	$\{0.01, 0.4, 0.8, 1.2\}$
Overhand Depth South	$\{0.01, 0.4, 0.8, 1.2\}$
Overhand Depth East	$\{0.01, 0.4, 0.8, 1.2\}$
Overhand Depth West	$\{0.01, 0.4, 0.8, 1.2\}$
Building Fabrics	$\{BF1, BF2, BF3, BF4, BF5\}$
Glazing Fabrics	$\{GF1, GF2, GF3, GF4, GF5\}$

The different retrofitting options for our experimental setup are summarized in Table 2.

Hierarchical clustering and Koopman modes

Given a full-scale zonal model and a representative data-set consisting of a zone's level output variable (for example, air temperature for all zones) on which zoning reduction relies: (1) in Hierarchical clustering approach, substantial recreations of intermediate zonal models are required, before the recreation of the final speedup model that consists of the desired number of zones; (2) in Koopman modes approach, a zoning approximation, where Equations 8 and 9 hold for a predefined Koopman modes of interest number, is used to recreate the final speedup model. In both approaches, recreation of a thermal simulation model is required, a tedious, slow and error-pruning process, commonly performed by a thermal simulation modeler manually. The benefit of an automatic process for generating speedup models based on zoning reduction approaches would be twofold: (1) it would be orders of magnitude faster than manually recreating building geometry; and (2) it would be less susceptible to human error.

Towards this direction, the three stages process presented in Figure 3 is proposed, utilizing EnergyPlus (Crawley et al., 2001) as the simulation engine to develop zonal models. In Stage 1, the objects of the

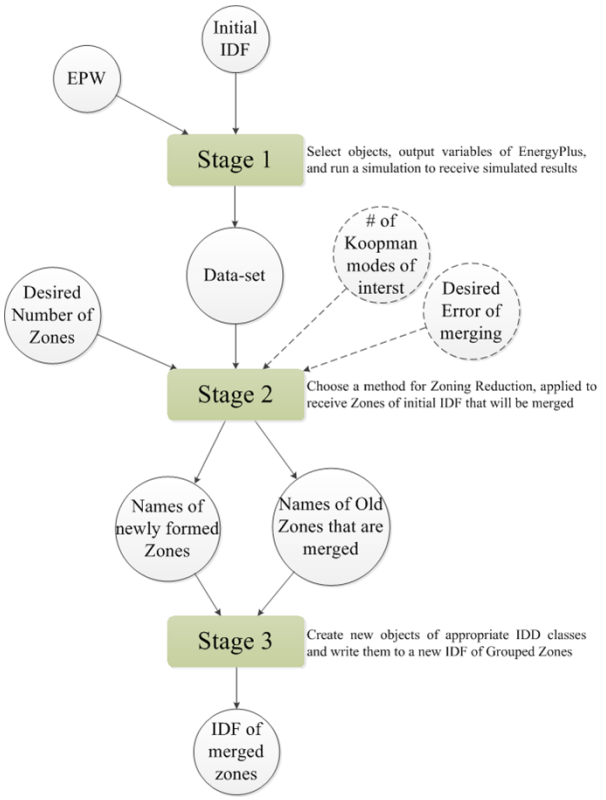

Figure 3: An overview of the automatic process for generating speedup model based on zoning reduction approaches

data-set, output variables of EnergyPlus, are defined and a full-scale zonal model (initial model) simulation is performed to receive simulated results.

In EnergyPlus, model input data are supplied by two ASCII (text) files: the Input Data Dictionary (IDD) and the Input Data File (IDF). All possible EnergyPlus classes, and a specification of the properties each class has, are defined in the IDD file, while an IDF file consists of all the necessary IDD classes' objects to properly define a thermal simulation model of a certain building. Each thermal simulation model has a different IDF file. This information is parsed by two Matlab scripts: the first script identifies the version of the IDF file, parses the appropriate IDD file, and creates a library ($\text{MatlabIDD}_{\text{xx}}$, where xx is the EnergyPlus version) of Matlab classes, corresponding to EnergyPlus classes; the second script identifies the version of a certain IDF file and parses this file conducing to $\text{MatlabIDD}_{\text{xx}}$ objects definition.

Beyond a wide variety of EnergyPlus output variables, particular variables can be reported depending on the actual simulation problem described in the IDF. The Report Data Dictionary (RDD) is a text file listing those variables available for reporting during the simulation of a certain IDF, including possible objects of the data-set required for a zoning reduction approach execution. For instance, Fanger Predicted Mean Vote (PMV) could not be reported, if People class objects for all zones have not been defined. Selecting a zone's level output variable from that list, an object of the *Output:Variable* class is defined and imported in the initial IDF. A plethora of zone's level output variables could exist in the RDD file, commonly including zone air temperature, zone operative temperature and zone relative humidity to name but a few.

After an initial IDF — enriched with the selected *Output:Variable* — simulation run, the resulted data-set of the selected variable is printed in a comma separated text by a semi column, where each column corresponds to a unique zone's variable time-series (zone air temperature with reporting frequency equal to the simulation timestep). The order of columns is not predefined, while the user is not allowed to set a preferable order. To overcome such a limitation, EnergyPlus could be used in conjunction with the Building Controls Virtual Test Bed (Wetter, 2011).

To configure the data exchange between EnergyPlus and Matlab through BCVTB, the following four steps are required: (1) enrich the initial IDF with the selected *Output:Variable* object and an object of the *ExternalInterface* class; (2) develop an xml file, named variables.cfg, that defines the mapping between EnergyPlus and BCVTB variables; (3) create an m file, named simulateAndExit.m, to determine the data exchange between MATLAB and the BCVTB variables; and (4) create a Ptolemy model.

In order to automatically create — when required — the enriched IDF, the variables.cfg and the simulateAndExit.m files, three respective Matlab scripts have been developed.

The data-set consisting of the simulated results (outputs of Stage 1) along with the desired number of zones, or the desired errors of zones' merging ϵ_1, ϵ_2 and the Koopman modes of interest number, are forwarded to Stage 2, where a zoning reduction approach is chosen and is applied to receive groups of zones that will be merged.

Names of newly formed zones and names of initial model's zones that belong to each newly formed zone, are finally used to automatically recreate the final speedup model in Stage 3, in the following manner:

- For each newly formed zone, a new object of the *Zone* class is determined.
- When zones are merged forming a new zone, shared walls and openings (doors, windows) are no more *BuildingSurface:Detailed* and *FenestrationSurface:Detailed* class objects, respectively, but *InternalMass* class objects acting as thermal mass for the new zone. Moreover, internal loads from electric-equipment, lighting, and occupancy, objects of *ElectricEquipment*, *Lights* and *People* classes, respectively, are combined for the newly formed zone. With the initial IDF parsed objects of *BuildingSurface:Detailed*, *FenestrationSurface:Detailed*, *In-*

ternalMass, *ElectricEquipment*, *Lights* and *People* classes as inputs, a Matlab script has been developed and is applied to properly determine new objects of these classes.

- For each new object of *Zone*, *BuildingSurface:Detailed*, *FenestrationSurface:Detailed*, *InternalMass*, *ElectricEquipment*, *Lights* and *People* classes the respective class "write" method is called, implementing the writing operations performed on objects of the corresponding class to create the new IDF of merged zones.

A set of experiments (referred as experiments' set 1 in the results section) was performed for each zoning reduction methodology, selecting as data-set the simulated zones' air temperature. A whole year simulation time interval is selected, while assuming all zones to be free floating, the conditions during this period are as follows: internal gains, infiltration and ventilation are identical for all zones; and there is no HVAC system available to control the zone air temperature.

Towards investigating the impact of the generated zoning approximations on model accuracy, a uniform criterion is used, the building's Heating/Cooling (H/C) energy demands. Here, all zones of each evaluated speedup model are simulated for a whole year simulation time interval. The accuracy of a speedup model is measured by comparing the total energy demands, where the conditions during this period are as follows: internal gains, infiltration and ventilation are identical for all zones; and an ideal HVAC system is available at each zone, controlled by a dual setpoint temperature sensor, where heating and cooling setpoint temperatures were set to 21°C and 23°C, respectively.

The prediction accuracy of each zoning approximation on the H/C energy demands under different, passive retrofitting scenarios (see Table 2 excluding the HVAC type parameter), in terms of the Mean Absolute Percentage Error (MAPE), was also investigated, where both the full-scale model (25 zones) and a group of reduced models – with 20 zones and 15 zones – were simulated for a whole year time interval (referred as experiment set 2 in the results section). The simulation models under certain passive retrofitting scenarios (see Table 2) were generated utilizing the jEPlus tool (Zhang and Korolija, 2010).

The principal limitation in the applicability of such methodologies stems from the lack of knowledge on how the zones' merging should be performed when different types of zone level HVAC systems operate to heat/cool the zones. Investigating the aforementioned limitation, a further set of experiments (referred as experiments' set 3 in the results section) was conducted, where the ideal HVAC systems were replaced by VAV systems, described above. Concerning the zone level HVAC system, zone's merging is performed in the following manner: when zones are merged forming a new zone, a list of zone level systems is generated (following the *ZoneHVAC:EquipmentList* structure of EnergyPlus).

GP meta-models

Following the parameter list and values of the different retrofitting options for our experimental setup (see Table 2), the goal is to construct a meta-model that will be trained in a "small" sample of different combinations and will be able to predict the annual heating and cooling energy consumption, for any combination of these parameters. In order to generate different samples, a jEPLus (Zhang and Korolija, 2010) project is defined and Latin Hypercube Sampling (LHS) is selected as our sampling methodology. Here, following the paradigm of Symonds et al. (2016), we have developed three GP meta-models, one for each different system, instead of one large meta-model. This approach, apart from reducing the computational burden, does not necessitate the re-generation of the entire meta-model in case more HVAC systems are added in the retrofitting options. Regarding the Building and Glazing Fabrics variables, instead of treating them as classical categorical variables and apply methods such as "one-hot" encoding, we argue that there is a notion of ordering here (we move from non-insulation to best-practice fabrics) and we encode this ordering using a simple linear mapping: $\{\text{BF1/GF1} \rightarrow 0, \ldots, \text{BF5/GF5} \rightarrow 4\}$. In addition, we normalize both the parameters and the target variables (heating and cooling energy consumption) in $[0, 1]$.

For the GP parametrization, we used a composite covariance function, comprising of the addition of an Rational Quadratic and a Matérn covariance function with $\nu = \frac{1}{2}$. For both covariance functions we used Automatic Relevance Determination (ARD) Rasmussen and Williams (2006), meaning that a different length-scale was defined for each dimension of the parameter space. The definition of the GPs and the optimization of the hyperparameters were performed using the GPML Matlab toolbox.[1]

Results

Hierarchical clustering and Koopman modes

Evaluating the proposed automatic process, the main positive result is that both zoning reduction methodologies led to the same zoning approximations, confirming thereby the effectiveness of the Hierarchical Clustering approach, since the Koopman Modes approach has been verified in the context of a recent work (Georgescu and Mezić, 2015). For intuition on how those approaches reduce the number of zone, the 3D geometries of the 25 zones (the initial full-scale model), 24 zones and 23 zones models are depicted in Figure 4.

Although both zoning reduction approaches are

[1] http://www.gaussianprocess.org/gpml/code/matlab/doc/

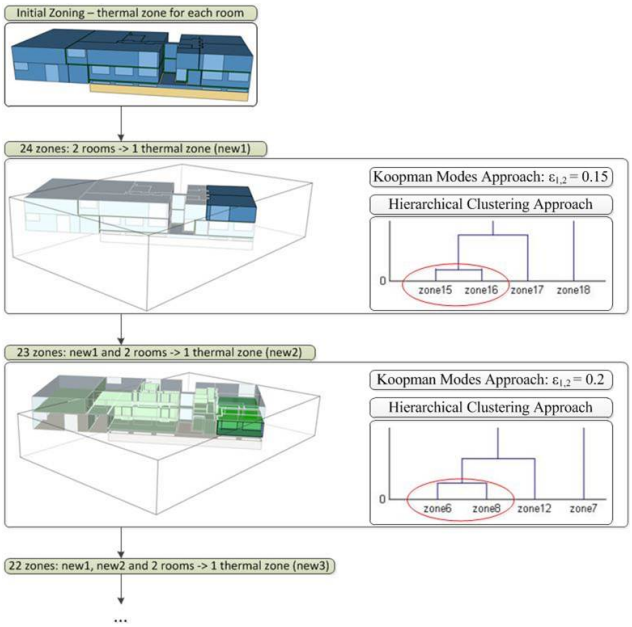

Figure 4: Zoning approximations for the first two steps of Hierarchical Clustering methodology and the respective $\epsilon_{1,2}$ values of Koopman Modes methodology

equally effective, the ease of use of the Hierarchical clustering approach lies in the fact that the only input to the algorithm is the desired number of zones; in contrast, the difficulty of use of the Koopman Modes approach lies in the difficulty of selecting proper values of ϵ_1, ϵ_2 and the number of modes of interest, since such selection does not have a physical interpretation, but it is based on experience the modeler has with this approach.

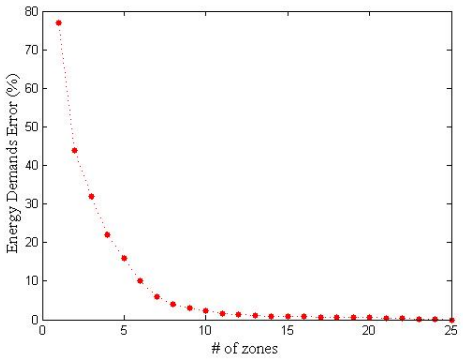

Figure 5: H/C energy demands' error in prediction as the number of zones increases

According to Figure 5, the H/C energy demands' error in prediction is inversely proportional to the number of zones.

Table 3 summarizes the three set of experiments' results, which were performed to evaluate the effectiveness of zoning reduction methodologies. Concerning the experiments' set 1, for the Koopman modes approach, setting the number of Koopman modes of interest to 10 constantly, as increased values of ϵ_1 and ϵ_2 are used to check if Equations 8 and 9 hold, more zones are determined to be sufficiently similar to each other, reducing the total number of zones. As the number of zones decreases, the calculated H/C energy demands' error increases, while the simulation runtime decreases. In words of the Hierarchical clustering approach, as the desired number of zones decreases, the model's accuracy decreases, while the simulation is less computationally expensive.

Table 3: Accuracy of Hierarchical clustering and Koopman modes methodologies

# of experim. set		**# of zones**		
		25	20	15
1	$\epsilon_{1,2}$	0	0.3	0.68
	MAPE (%)	0	0.386	0.793
	Runtime (sec)	93	76	51
2	MAPE (%)	0	0.397	0.815
3	MAPE (%)	0	1.375	3.218

The experiments' set 2 results demonstrate the effectiveness of each zoning approximation to predict the H/C energy demands under 1200 different, passive retrofit scenarios, in terms of the Mean Absolute Percentage Error (MAPE), while results of the experiments' set 3 make obvious the inapplicability of the zoning reduction methodologies in cases where actual HVAC systems operate to condition the zones. An explanation for the increased values of MAPE could be the way that the zone's merging is performed, regarding the zone level HVAC system: utilizing the *ZoneHVAC:EquipmentList*, an equipments' sequence for heating and cooling is defined, where the first sequence equipment tries to meet the entire demand with its capacity and then pass the results on to the second and so on for both heating and cooling. Such a definition differs from how multiple HVAC system operate in parallel (actual case) to meet the demand.

GP meta-models

As an illustration of the potential of the approach, we sampled 12,000 combinations per HVAC system using LHS and used 90% of these samples for training the meta-model and 10% of the samples to test the model accuracy. In contrast to the findings of Symonds et al. (2016), we observed (as also discussed in Safarzadegan Gilan et al. (2016)) that increasing the number of samples leads to better approximations. Indeed, the correlation coefficient (R^2) and the Mean Absolute Percentage Error (MAPE), shown in Table 4, indicate an excellent performance of the meta-model.

Conclusion

In the present work, three simulation-time reduction techniques (Hierarchical clustering, Koopman Modes, and GP meta-modeling) are evaluated in terms of their effectiveness to predict the heating/cooling en-

Table 4: Accuracy of GP meta-models

System	Cooling		Heating	
	R^2	MAPE	R^2	MAPE
VAV	0.999	0.0055	0.999	0.0210
CAV	0.999	0.0110	0.999	0.0015
FC	0.999	0.0058	0.999	0.0020

ergy demands/consumption under different retrofit scenarios.

All of them have proven to be viable options for simulation-time reduction. For the zoning reduction approaches, both methodologies led to the same zoning approximations, thus confirming the viability of the Hierarchical Clustering approach, since the Koopman Modes approach has been verified in the context of a recent work (Georgescu and Mezić, 2015).

The main advantage of the GP meta-model approach over the zoning reduction techniques stems from the fact that this approach does not necessitate any on-the-fly modifications of the simulation models – a task that proved to be quite difficult due to the automatic zoning of the HVAC systems. Future work will investigate alternatives on how the automatic zoning of the HVAC systems should be performed.

Another critical difference between the two approaches is the treatment of the simulation model output used as similarity measure in the Hierarchical Clustering and Koopman Modes approaches and as target variable on the GP meta-modeling methodology. In the first two approaches, only one variable can be used for determining similarity between zones (e.g. the energy consumption or the operative temperature of each zone). On the other hand, the GP meta-modeling approach offers significantly more flexibility, since different meta-models can be created for several target variables. These meta-models can in turn be used as inputs to optimization setups that utilize more than one variables, such as multi-objective and constrained optimization applications.

On the downside, the GP approach also has its limitations. The main problem is the selection of a proper covariance function, which is a non-trivial task requiring a laborious fine-tuning process. Here, a notable ongoing effort towards automating this process has been performed under the Automatic Statistician Project (Duvenaud, 2014). Another downside of the GP meta-modeling methodology (and of several Machine Learning approaches in general) is determining the number of samples required for an accurate approximation. Each problem is different and there are no guidelines on selecting an "optimal" number of samples depending on the dimension of the parameter space and the expected accuracy. This problem becomes even more critical due to the high time complexity of the approach ($\mathcal{O}(n^3)$ for exact inference). Here, future work will focus on evaluating different approximation methods for large-scale GP regression Quinonero-Candela et al. (2007).

Overall, the idea of applying simulation-time reduction methodologies to reduce the computational effort in tasks facilitating a large number of calls to a detailed simulation model of a building – like discovering the best retrofitting strategy – has proven to be valid. One of the most powerful features of the proposed approach is that is applicable to any building, regardless of its individual characteristics, like e.g. geometry, construction, climate, usage, type, etc. To add to this, the three-stage automatic model (re-)generation process developed here (Figure 3) for the Hierarchical Clustering and Koopman Modes approaches is able to address any clustering/zone merging (geometric) requirements seamlessly, but requires some further customization to be able to cope with the merging of HVAC zones for different types of HVAC systems.

Acknowledgements

The research leading to these results has been partially funded by the European Commission FP7-ICT-2011-6, ICT Systems for Energy Efficiency under contract #288409 (BaaS).

Georgios Giannakis and Dimitrios Rovas gratefully acknowledge financial support from the European Commission H2020-EeB5-2015 project "Optimised Energy Efficient Design Platform for Refurbishment at District Level" under contract #680676 (OptEEmAL).

Georgios Kontes gratefully acknowledges financial support from MOEEBIUS project, a Horizon 2020 research and innovation program under grant agreement #680517, as well as the use of the services and facilities of the Energie Campus Nürnberg and financial support through the "Aufbruch Bayern (Bavaria on the move)" initiative of the state of Bavaria.

References

ASHRAE 90.1 (2010). Energy standard for buildings except low-rise residential buildings. *ASHRAE/IESNA Standard 90*(1).

Bazjanac, V. (2008). IFC BIM-based methodology for semi-automated building energy performance simulation. *Lawrence Berkeley National Laboratory*.

Brochu, E., M. Cora, and N. de Freitas (2009). A Tutorial on Bayesian Optimization of Expensive Cost Functions, with Application to Active User Modeling and Hierarchical Reinforcement Learning. Technical report, TR-2009-023, Department of Computer Science, University of British Columbia.

Crawley, D. et al. (2001). EnergyPlus: creating a new-generation building energy simulation program. *Energy and Buildings 33*(4), 319–331.

Duvenaud, D. (2014). *Automatic Model Construction with Gaussian Processes*. Ph. D. thesis, Computa-

tional and Biological Learning Laboratory, University of Cambridge.

Duvenaud, D., J. R. Lloyd, R. Grosse, J. B. Tenenbaum, and Z. Ghahramani (2013, June). Structure Discovery in Nonparametric Regression through Compositional Kernel Search. In *Proceedings of the 30th International Conference on Machine Learning*, pp. 1166–1174.

Forrester, A., A. Sobester, and A. Keane (2008). *Engineering design via surrogate modelling: a practical guide*. John Wiley & Sons. ISBN: 9780470060681.

Georgescu, M. and I. Mezić (2015). Building energy modeling: A systematic approach to zoning and model reduction using Koopman Mode Analysis. *Energy and Buildings 86*, 794–802.

Giannakis, G., G. Lilis, M. Garcia, G. Kontes, C. Valmaseda, and D. Rovas (2015). A Methodology to Automatically Generate Geometry Inputs for Energy Performance Simulation from IFC BIM Models. In *Proceedings of the Building Simulation 2015: 14th Conference of the International Building Performance Simulation Association*, pp. 504–511.

Giannakis, G., M. Pichler, G. Kontes, H. Schranzhofer, and D. Rovas (2013). Simulation speedup techniques for computationally demanding tasks. In *Proceedings of the Building Simulation 2013: 13th Conference of the International Building Performance Simulation Association*, pp. 3761–3768.

Korolija, I., L. Marjanovic-Halburd, Y. Zhang, and V. I. Hanby (2013a). UK office buildings archetypal model as methodological approach in development of regression models for predicting building energy consumption from heating and cooling demands. *Energy and Buildings 60*, 152–162.

Korolija, I., Y. Zhang, L. Marjanovic-Halburd, and V. I. Hanby (2013b). Regression models for predicting UK office building energy consumption from heating and cooling demands. *Energy and Buildings 59*, 214–227.

Lilis, G. N., G. I. Giannakis, and D. V. Rovas (2016). Automatic generation of second-level space boundary topology from IFC geometry inputs. *Automation in Construction*.

Magnier, L. and F. Haghighat (2010). Multiobjective optimization of building design using TRNSYS simulations, genetic algorithm, and Artificial Neural Network. *Building and Environment 45*(3), 739–746.

Maimon, O. and L. Rokach (2005). *Data mining and knowledge discovery handbook*, Volume 2. Springer. ISBN: 9780387098227.

Mezić, I. (2005). Spectral properties of dynamical systems, model reduction and decompositions. *Nonlinear Dynamics 41*(1-3), 309–325.

Quinonero-Candela, J., C. E. Rasmussen, and C. K. Williams (2007). Approximation methods for gaussian process regression. *Large-scale kernel machines*, 203–224.

Rasmussen, C. and C. K. I. Williams (2006). *Gaussian processes for machine learning*. Cambridge, Mass.: MIT Press. ISBN: 9780262182539.

Safarzadegan Gilan, S., N. Goyal, and B. Dilkina (2016). Active Learning in Multi-objective Evolutionary Algorithms for Sustainable Building Design. In *Proceedings of the 2016 on Genetic and Evolutionary Computation Conference*, pp. 589–596. ACM.

Scholkopf, B. and A. J. Smola (2001). *Learning with kernels: support vector machines, regularization, optimization, and beyond*. MIT press. ISBN: 9780262194754.

Susuki, Y. and I. Mezic (2010). Nonlinear koopman modes of coupled swing dynamics and coherency identification. In *Power and Energy Society General Meeting, 2010 IEEE*, pp. 1–8. IEEE.

Symonds, P., J. Taylor, Z. Chalabi, A. Mavrogianni, M. Davies, I. Hamilton, S. Vardoulakis, C. Heaviside, and H. Macintyre (2016). Development of an England-wide indoor overheating and air pollution model using artificial neural networks. *Journal of Building Performance Simulation*, 1–14.

Wetter, M. (2011). Co-simulation of building energy and control systems with the Building Controls Virtual Test Bed. *Journal of Building Performance Simulation 4*(3), 185–203.

Zhang, R., F. Liu, A. Schoergendorfer, Y. Hwang, Y. M. Lee, and J. L. Snowdon (2013). Optimal selection of building components using sequential design via statistical surrogate models. In *Proceedings of Building Simulation*, pp. 2584–2592.

Zhang, Y. and I. Korolija (2010). Performing complex parametric simulations with jEPlus. In *SET2010 – 9th International Conference on Sustainable Energy Technologies, Shanghai, China.*